^{13}C-Enriched Ribonucleosides: Synthesis and Application of ^{13}C-^{1}H and ^{13}C-^{13}C Spin-Coupling Constants To Assess Furanose and *N*-Glycoside Bond Conformations

Paul C. Kline and Anthony S. Serianni*

Contribution from the Department of Chemistry and Biochemistry, University of Notre Dame, Notre Dame, Indiana 46556. *Received October 4, 1989*

Abstract: Adenosine (**1**), cytidine (**2**), guanosine (**3**), and uridine (**4**) have been prepared chemically with ^{13}C enrichment (99 atom %) at C1′ and C2′ of the ribose ring. Reliable synthetic protocols have been developed to permit access to millimole quantities of labeled ribonucleosides required for structural studies of stable isotopically labeled oligonucleotides and for in vivo metabolism studies. High-resolution ^{1}H and ^{13}C NMR spectra of the enriched ribonucleosides have been obtained, and ^{13}C-^{13}C and ^{13}C-^{1}H spin-coupling constants have been measured for pathways within the β-D-ribofuranose ring and across the *N*-glycoside bond. Related couplings were determined in methyl α- and β-D-ribofuranosides (**5**, **6**), and in two conformationally constrained nucleosides, 2,2′-anhydro-(1-β-D-arabinofuranosyl)uracil (**7**) and 2′,3′-*O*-isopropylidene-2,5′-*O*-cyclouridine (**8**). The latter data were used to construct a crude Karplus curve for the ^{13}C-C-N-^{13}C coupling pathway across the *N*-glycoside bond in **1**-**4**. ^{1}H-^{1}H, ^{13}C-^{1}H, and ^{13}C-^{13}C coupling data are used to evaluate current models describing the conformational dynamics of **1**-**4** in aqueous solution.

Introduction

The ribonucleosides, adenosine (**1**), cytidine (**2**), guanosine (**3**), and uridine (**4**) (Chart I), are the building block molecules of ribonucleic acid (RNA) and have been the focus of numerous NMR studies since the original work by Jardetzky[1] and Lemieux.[2] These compounds contain structural domains defining hydroxymethyl, furanose ring, and *N*-glycoside bond conformation, and nuclear magnetic resonance (NMR) spectroscopy,[3-5] X-ray crystallography,[6] and potential energy and quantum mechanics calculations[7-9] are among the experimental and computational techniques employed to study these conformational features. NMR parameters have been most valuable in conformational studies of **1**-**4** in solution; for example, three-bond (vicinal) ^{1}H-^{1}H spin-coupling constants ($^{3}J_{HH}$) have been used extensively to characterize the structures of **1**-**4**, and several models based on these couplings have been proposed to describe ribofuranose and hydroxymethyl conformation and dynamics.[10,11]

The use of $^{3}J_{HH}$ to assess ribonucleoside conformation in solution is not without limitations. Models describing ribofuranose conformation, for example, rely on three intra-ring $^{3}J_{HH}$ values ($^{3}J_{H1',H2'}$, $^{3}J_{H2',H3'}$, $^{3}J_{H3',H4'}$) to define the five interdependent endocyclic torsion angles. In light of the well-known conformational flexibility of the furanose ring, these couplings provide minimal information with which to test the wide range of conformational options available to the molecule. In response to this problem, Serianni and Barker[12] and Cyr and Perlin[13] have argued that intra-ring vicinal ^{13}C-^{1}H and ^{13}C-^{13}C spin couplings may improve the conformational analysis of simple and complex furanoses and furanosides by providing more parameters to test conformational models. In this report, we extend these earlier studies to the four ribonucleosides **1**-**4** (Chart I), which have been singly labeled with ^{13}C at C1′ and C2′. High-resolution ^{1}H and ^{13}C NMR spectra have been obtained, and ^{13}C-^{1}H and ^{13}C-^{13}C spin-coupling constants have been measured within the ribofuranose ring and across the *N*-glycoside bond. A semiquantitative examination of the application of these couplings to ribonucleoside conformational analysis is presented. The utility of ^{13}C labels as structural probes in more complex molecules (e.g., oligonucleotides) is also discussed.

Methods and Instrumentation

Materials. Potassium [^{13}C]cyanide ($K^{13}CN$, 99 atom % ^{13}C) and deuterium oxide ($^{2}H_2O$, 99 atom % ^{2}H) were purchased from Cambridge Isotope Laboratories. Hexamethyldisilazane (HMDS) was purchased from Pierce Chemical Co. Trimethylsilyl trifluoromethanesulfonate, anhydrous 1,2-dichloroethane, hexamethylphosphoramide, diethyl azodicarboxylate, diphenyl carbonate, *p*-toluenesulfonic acid monohydrate, triphenylphosphine, Dowex ion-exchange resins, and 3-Å molecular sieves were obtained from Aldrich Chemical Co. Anhydrous ammonia was purchased from Linde/Union Carbide. Uracil, cytosine, N^2-acetylguanine, N^6-benzoyladenine, uridine, adenosine, guanosine, cytidine, methyl β-D-ribofuranoside, 1-*O*-acetyl 2,3,5-tri-*O*-benzoyl-β-D-ribofuranoside (ABR), 2,2′-anhydro-(1-β-D-arabinofuranosyl)uracil, 2′,3′-*O*-isopropylideneuridine, and 5% palladium on barium sulfate (Pd-$BaSO_4$) were purchased from Sigma Chemical Co. Silica gel 60 PF_{254} for radial chromatography was purchased from EM Reagents.

Pyridine was dried over KOH pellets for 1 week, distilled (bp 115-116 °C), and stored over 3-Å molecular sieves. Tetrahydrofuran was distilled (bp 66-67 °C) and stored over 3-Å molecular sieves. Ethyl orthoformate was purchased from Aldrich Chemical Co. and distilled prior to use (bp 145-146 °C). D-Erythrose was prepared by periodate cleavage of 4,6-*O*-ethylidene-D-glucose.[14] All other chemicals were reagent grade and were used without further purification. Melting points (uncorrected) were determined on a Mel-Temp apparatus.

Instrumentation. High-resolution ^{1}H NMR and ^{1}H-decoupled ^{13}C NMR spectra were obtained on a Nicolet NT-300 FT-NMR spectrometer equipped with quadrature-phase detection and a 293B pulse programmer. Sweep widths and digitizations of 1500 Hz and 16K data points, and 8200 Hz and 64K data points, were used for ^{1}H and ^{13}C spectra, respectively. Free induction decays were zero-filled to 32K and

(1) (a) Jardetzky, C. D. *J. Am. Chem. Soc.* **1960**, *82*, 229. (b) Jardetzky, C. D. *J. Am. Chem. Soc.* **1962**, *84*, 62.
(2) Lemieux, R. U. *Can. J. Chem.* **1961**, *39*, 116.
(3) Van de Ven, F. J. M.; Hilbers, C. W. *Eur. J. Biochem.* **1988**, *178*, 1.
(4) (a) Davies, D. B. *Prog. Nucl. Magn. Reson. Spectrosc.* **1978**, *12*, 135. (b) Remin, M. *J. Biomol. Struct. Dyn.* **1984**, *1*, 211.
(5) de Leeuw, F. A. A. M.; Altona, C. *J. Chem. Soc., Perkin Trans. 2* **1982**, 375.
(6) Sundaralingam, M. *Ann. N.Y. Acad. Sci.* **1975**, *3*, 255.
(7) (a) Berthod, H.; Pullman, B. *Biochim. Biophys. Acta* **1971**, *232*, 595. (b) Lesyng, B.; Marck, C.; Guschlbauer, W. *Int. J. Quantum Chem.* **1985**, *28*, 517.
(8) (a) Schlick, T.; Peskin, C.; Broyde, S.; Overton, M. *J. Comput. Chem.* **1987**, *8*, 1199. (b) Olson, W. *J. Am. Chem. Soc.* **1982**, *104*, 278. (c) Pearlman, D. A.; Kim, S.-H. *J. Biomol. Struct. Dyn.* **1985**, *3*, 99.
(9) (a) Levitt, M.; Warshel, A. *J. Am. Chem. Soc.* **1978**, *100*, 2607. (b) Harvey, S. C.; Prabhakaran, M. *J. Am. Chem. Soc.* **1986**, *108*, 6128. (c) Wiorkiewicz-Kuczera, J.; Rabczenko, A. *J. Chem. Soc., Perkin Trans. 2* **1986**, 437.
(10) de Leeuw, H. P. M.; Haasnoot, C. A. G.; Altona, C. *Isr. J. Chem.* **1980**, *20*, 108.
(11) (a) Davies, D. B.; Rabzcenko, A. *J. Chem. Soc., Perkin Trans. 2* **1975**, 1703. (b) Kline, P. C.; Serianni, A. S. *Magn. Reson. Chem.* **1988**, *26*, 120.
(12) Serianni, A. S.; Barker, R. *J. Org. Chem.* **1984**, *49*, 3292.
(13) Cyr, N.; Perlin, A. S. *Can. J. Chem.* **1979**, *57*, 2504.
(14) Perlin, A. S. *Methods Carbohydr. Chem.* **1962**, *1*, 64.

0002-7863/90/1512-7373$02.50/0

Chart I

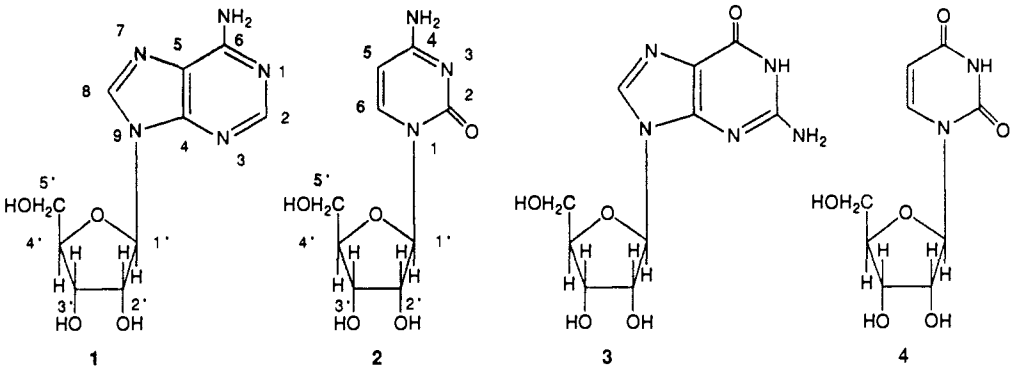

1 2 3 4

128K data points for ^1H and ^{13}C spectra, respectively, prior to Fourier transformation. Spectra were processed with a double-exponential filter (resolution enhancement) chosen empirically to maximize resolution.

2D ^{13}C–^1H chemical shift correlation spectroscopy was conducted on a General Electric GN-300 FT-NMR spectrometer equipped with quadrature-phase detection and a 293B pulse programmer. The experiment was implemented with the CSCMR pulse program provided by G. E. NMR Systems.

Synthesis of D-[^{13}C]Ribose and Methyl β-D-[^{13}C]Ribofuranoside (6). D-[1-^{13}C]Ribose and D-[1-^{13}C]arabinose were synthesized from D-erythrose by the cyanohydrin reduction method of Serianni et al.[15] After purification, D-[1-^{13}C]arabinose was converted to D-[2-^{13}C]ribose by molybdate-catalyzed epimerization.[16] D-[1-^{13}C]Arabinose (19.2 g, 128 mmol) was dissolved in dimethylformamide (1300 mL), molybdenyl acetylacetonate (2.1 g, 6.4 mmol) was added, and the solution was stirred for 24 h at 50 °C. The reaction mixture was cooled to 5 °C, two volumes of water were added, and the solution was extracted twice with two volumes of methylene chloride. The aqueous phase was deionized by separate, batchwise treatments with excess Dowex 50 × 8 (20–50 mesh) in the H^+ form and Dowex 1 × 8 (20–50 mesh) in the acetate form. The solution was concentrated to a syrup and applied to a column (83 cm × 15 cm) of Dowex 50 × 8 (200–400 mesh) resin in the Ca^{2+} form.[17] The column was eluted with distilled water at a rate of 1.5 mL/min. Fractions (15 mL) were collected and assayed for sugar with phenol–sulfuric acid.[18] Fractions 311–640 (D-[1-^{13}C]arabinose) and 892–1214 (D-[2-^{13}C]ribose) were pooled and concentrated in vacuo at 30 °C, and the pentoses were quantified by titration with iodine:[19] yield D-[1-^{13}C]-arabinose, 10.2 g, 67.5 mmol, 53%; D-[2-^{13}C]ribose, 5.1 g, 33.8 mmol, 26%. The epimerization was repeated twice to increase the yield of D-[2-^{13}C]ribose to 9.1 g (60.2 mmol; overall yield, 47%).

^{13}C-labeled D-riboses were converted to a mixture of methyl α- and β-D-[^{13}C]ribofuranosides as described by Barker and Fletcher.[20a] D-[^{13}C]Ribose (15.1 g, 100 mmol) was evaporated three times from 50 mL of anhydrous methanol at 30 °C in vacuo. The resulting syrup was dissolved in 300 mL of anhydrous methanol and cooled to 4 °C. Concentrated sulfuric acid (1.5 mL) was added, and the reaction mixture was stirred for 14 h at 4 °C. The acid was neutralized by passage of the reaction mixture through a column of Amberlite IRA-68 resin in the OH^- form (40 g of resin/mL of H_2SO_4) packed in anhydrous methanol. The column was eluted with anhydrous methanol until the phenol–sulfuric acid assay[18] was negative. The solvent was evaporated in vacuo at 30 °C, and the anomers were separated by chromatography on a column (118 cm × 2.5 cm) of Dowex 1 × 2 (200–400 mesh) ion-exchange resin in the hydroxide form.[20b] The column was eluted with CO_2-free water at a rate of 1.2 mL/min, and fractions (21 mL) were collected and assayed with phenol–sulfuric acid.[18] Fractions 56–93 and 110–257 were pooled, concentrated in vacuo at 30 °C, and analyzed by ^{13}C NMR. Fractions 56–93 contained the α-anomer **5** and fractions 110–257 contained the β-anomer **6**, as established from their characteristic ^1H and ^{13}C NMR spectra:[12,21] yield α, 3.9 g, 24 mmol, 24%; β, 11.7 g, 71 mmol, 71%. Anomerization of the α-anomer using the original reaction conditions improved the yield of the desired β-anomer. The β-anomer was crystallized by adding a seed crystal to the syrup, and crystalline methyl β-D-[^{13}C]ribofuranoside (**6**) was dried under vacuum at 50 °C prior to use in ribonucleoside syntheses.

Synthesis of 1-*O*-Acetyl 2,3,5-Tri-*O*-benzoyl-β-D-[^{13}C]ribofuranoside (ABR).[22] Methyl β-D-[^{13}C]ribofuranoside (**6**; 4.9 g, 30 mmol) was dissolved in anhydrous pyridine (20 mL) in a 250-mL round-bottom flask and the solvent evaporated in vacuo at 30 °C. This procedure was repeated twice to remove residual water. The resulting syrup was dissolved in a mixture of anhydrous pyridine (53 mL) and chloroform (25 mL), the reaction flask was cooled in an ice bath, and benzoyl chloride (17.5 mL, 150 mmol) was added dropwise through an equilizing funnel with stirring. After 12 h at 4 °C, crushed ice (3 g) was added and the mixture was stirred for 2 h at room temperature to hydrolyze unreacted benzoyl chloride. The mixture was transferred to a separatory funnel, the organic phase was removed, and the aqueous phase was extracted twice with 300 mL of chloroform. The organic phases were combined and back-extracted with water (200 mL), and the organic phase was dried over anhydrous sodium sulfate.

The organic solvent was removed in vacuo (vacuum pump), and the residual stiff syrup was dissolved in glacial acetic acid (7.5 mL) and acetic anhydride (16.9 mL). The solution was cooled in an ice bath, and concentrated H_2SO_4 (2.4 mL) was added dropwise over 5 min. If crystallization did not occur within ~10 min after the complete addition of H_2SO_4, a small seed crystal of ABR was added. After crystallization, the reaction mixture was stored overnight at 4 °C. Crushed ice (24 g) was added, and the mixture was stirred for 30 min and extracted four times with 300 mL of chloroform. The combined chloroform extracts were washed with ice-cold saturated aqueous sodium bicarbonate until CO_2 evolution ceased, and the organic phase was dried over anhydrous sodium sulfate. The solvent was removed at 30 °C in vacuo, and the product was crystallized by concentrating the syrup from 100 mL of isopropyl alcohol several times. Recrystallization from isopropyl alcohol yielded white, needlelike crystals that were dried in vacuo at 50 °C: yield 10.3 g, 20.4 mmol, 68%; mp 130–131 °C (lit.[22] mp 128–130 °C); ^{13}C NMR (C^2HCl_3) δ 168.9, 165.9, 165.3, and 164.9 (C=O); 133.6, 133.5, 129.7, and 128.3 (Ar); 98.3 (C1′), 79.9 (C4′), 74.9 (C2′), 71.3 (C3′), 63.7 (C5′), 20.9 (CH_3).

Synthesis of Acylated Nitrogen Bases. N^6-Benzoyladenine and N^2-acetylguanine were obtained commercially. N^4-Acetylcytosine was prepared by the method of Codington and Fox.[23] Cytosine (5.5 g, 50 mmol) was refluxed in 140 mL of acetic anhydride for 4 h under a nitrogen atmosphere. The reaction mixture was stored overnight at 4 °C, during which time the product crystallized. The crystals were washed with cold ethanol and water and recrystallized from water: yield 5.8 g, 37.6 mmol, 75%; mp 328–329 °C (lit.[23] mp 326–328 °C dec).

General Procedure For the Preparation of ^{13}C-Labeled Ribonucleosides. ^{13}C-labeled ribonucleosides were synthesized as described by Vorbrüggen et al.[24] with some modifications. Before use, all nitrogen bases and ^{13}C-labeled ABR were dried in vacuo at 50 °C for 24 h, and glassware was dried overnight at 120 °C and cooled in a desiccator. The reaction vessel consisted of a 100-mL round-bottom flask with a stopcock-equipped sidearm, and a distilling head that allowed isolation of the receiver

(15) (a) Serianni, A. S.; Nunez, H. A.; Barker, R. *Carbohydr. Res.* **1979**, *72*, 71. (b) Serianni, A. S.; Barker, R. Synthetic Approaches to Carbohydrates Enriched with Stable Isotopes of Carbon, Hydrogen and Oxygen. In *Isotopes in the Physical and Biomedical Sciences*; Buncel, E., Jones, J. R., Eds.; Elsevier: New York, 1987; p 211.

(16) Hayes, M. L.; Pennings, N. J.; Serianni, A. S.; Barker, R. *J. Am. Chem. Soc.* **1982**, *104*, 6764.

(17) Angyal, S. J.; Bethell, G. S.; Beveridge, R. J. *Carbohydr. Res.* **1979**, *73*, 9.

(18) Hodge, J. E.; Hofreiter, B. T. *Methods Carbohydr. Chem.* **1962**, *1*, 380.

(19) Schaffer, R.; Isbell, H. S. *Methods Carbohydr. Chem.* **1963**, *2*, 11.

(20) (a) Barker, R.; Fletcher, H. G., Jr. *J. Org. Chem.* **1961**, *26*, 4605. (b) Austin, P. W.; Hardy, F. E.; Buchanan, J. G.; Baddiley, J. *J. Chem. Soc.* **1963**, 5350.

(21) Wu, G. D.; Serianni, A. S.; Barker, R. *J. Org. Chem.* **1983**, *48*, 1750.

(22) Recondo, E. F.; Rinderknecht, G. L. *Helv. Chim. Acta* **1959**, *42*, 1171.

(23) Codington, F.; Fox, J. J. *Methods Carbohydr. Chem.* **1963**, *2*, 113.

(24) Vorbrüggen, H.; Krolikiewicz, K.; Bennua, B. *Chem. Ber.* **1981**, *114*, 1234.

Table I. Reaction Conditions and Purification of Ribonucleosides **1–4**

compound	protected base	condenstn reactn time, h	silica gel solvent	deblocking reactn time, h	Dowex solvent	yield, %	mp, °C
adenosine (**1**)	N^6-benzoyladenine	5	90% CH_2Cl_2/ 10% MeOH	24	70% CO_2-free H_2O/30% MeOH (500 mL); 40% CO_2-free H_2O/60% MeOH (900 mL)	82	234–237
cytidine (**2**)	N^4-acetylcytosine	2	95% CH_2Cl_2/ MeOH	16	70% CO_2-free H_2O/30% MeOH (1400 mL)	95	214–216
guanosine (**3**)	N^2-acetylguanine	2		42	70% CO_2-free H_2O/30% MeOH (500 mL); 0.25 M TEAB,[b] pH 9 (900 mL)	*a*	252 (dec)
uridine (**4**)	uracil	4	75% CH_2Cl_2/ EtOAc	16	70% CO_2-free H_2O/30% MeOH (500 mL); 0.25 M TEAB,[b] pH 9 (900 mL)	89	167–169

[a] This yield varied from 20 to 65% (see text). [b] TEAB, triethylammonium bicarbonate.

flask. All reactions were conducted under an atmosphere of dry nitrogen.

The reaction vessel was assembled with 5.5 mmol of the appropriate base (Table I) in the reaction flask. After the vessel was purged three times with dry nitrogen, HMDS (25 mL) was added. For N^6-benzoyladenine and N^2-acetylguanine, anhydrous pyridine (0.5 mL) was added to accelerate silylation. The suspension was refluxed under dry nitrogen until the base completely dissolved (~4 h). Excess HMDS was then removed by distillation at atmospheric pressure, leaving a clear syrup. The receiver flask was isolated, removed, and replaced with a clean dry flask. To remove the last trace of HMDS, the syrup was heated at 50 °C in vacuo for 20 min. The vacuum was released by addition of dry nitrogen, [^{13}C]ABR (2.5 g, 5 mmol) dissolved in 50 mL of anhydrous 1,2-dichloroethane and trimethylsilyl trifluoromethanesulfonate (1.3 mL, 7 mmol) were added, and the reaction mixture was refluxed for the appropriate time (Table I).

After the condensation reaction was complete, the reaction mixture was cooled to room temperature and diluted with 100 mL of methylene chloride. The solution was extracted with 100 mL of ice-cold saturated aqueous sodium bicarbonate and the organic phase was dried over anhydrous sodium sulfate. The solvent was removed in vacuo at 30 °C, and the crude protected ribonucleoside was dissolved in 1–2 mL of methylene chloride and, with the exception of the guanosine derivative, purified in two batches by radial chromatography using a 4-mm-thick circular silica gel plate. The acylated ribonucleosides were eluted with the solvents given in Table I. Solvent and nitrogen flow rates during radial chromatography were 5 and 15 mL/min, respectively. The sample was detected under UV light (254 nm) as it eluted from the plate, and the main band was collected and concentrated in vacuo at 30 °C.

N^2-Acetyl-2′,3′,5′-tri-*O*-benzoylguanosine was purified by flash chromatography on silica gel.[25] The column was developed by using ethyl acetate, followed by 97% ethyl acetate–3% methanol. Fractions (18 mL) were collected and assayed by TLC using 90% acetonitrile–10% 1,4-dioxane. The main peak was pooled and concentrated in vacuo at 30 °C.

The acyl protecting groups were removed with methanolic ammonia, which was prepared by bubbling anhydrous ammonia through 50 mL of anhydrous methanol at 0 °C for 10 min. The acylated nucleoside was dissolved in freshly prepared methanolic ammonia and incubated at 25 °C for the reaction times given in Table I. The solvent was removed in vacuo at 30 °C and the residue dissolved in 100 mL of distilled water. The aqueous solution was extracted three times with 50 mL of chloroform and 50 mL of diethyl ether. The aqueous phase was concentrated in vacuo at 30 °C and the syrup applied to a 2 cm × 21 cm column containing Dowex 1 × 2 (200–400 mesh) resin in the OH^- form.[26] The effluent was monitored continuously at 254 nm by using an Isco UA-5 absorbance/fluorescence detector with a Type 6 optical unit. The column was washed with 30% methanol–70% CO_2-free distilled water, and the nucleosides were eluted with the solvents given in Table I. The main UV-absorbing peak was pooled and concentrated in vacuo at 30 °C. Triethylammonium bicarbonate (TEAB) buffer was removed from the uridine and guanosine preparations by repeated evaporation of water (100 mL) in vacuo at 30 °C.

Cytidine (**2**) and uridine (**4**) were recrystallized from hot ethanol, and adenosine (**1**) and guanosine (**3**) were recrystallized from hot distilled water. ^1H and ^{13}C NMR spectra of the [^{13}C]ribonucleosides were identical with those of authentic samples except for the expected additional signal multiplicity arising from ^{13}C–^1H and ^{13}C–^{13}C couplings, respectively.

Synthesis of 2,2′-Anhydro-(1-β-D-[2′-^{13}C]arabinofuranosyl)uracil (7).[27] [2′-^{13}C]Uridine (0.24 g, 1 mmol) was dissolved in 1 mL of hexamethylphosphoramide in a 3-mL Reacti-Vial (Pierce Chemical Co.). Diphenyl carbonate (0.3 g, 1.4 mmol) and sodium bicarbonate (6 mg) were added, and the solution was heated for 20 min at 150 °C. After being cooled, the mixture was poured into water (10 mL) and extracted three times with 10 mL of chloroform. The aqueous phase was concentrated in vacuo at 30 °C, and the product **7** was crystallized from methanol: yield 0.18 g, 0.8 mmol, 82%; mp 237–238 °C; ^1H NMR (^2H_2O) δ 3.55 and 3.56 (m, 2 H, H5′, H5″), 4.39 (m, 1 H, H4′), 4.66 (m, 1 H, H3′), 5.47 (m, 1 H, H2′), 6.18 (d, 1 H, H5), 6.53 (dd, 1 H, H1′), 7.91 (d, 1 H, H6).

Synthesis of 2′,3′-*O*-Isopropylidene-2,5′-*O*-[2′-^{13}C]cyclouridine (8). 2′,3′-*O*-Isopropylidene[2′-^{13}C]uridine was synthesized according to the procedure of Tomasz.[28] *p*-Toluenesulfonic acid monohydrate (0.19 g, 1 mmol) and [2′-^{13}C]uridine (0.24 g, 1 mmol) were suspended in 20 mL of acetone (the nucleoside must be added first), and ethyl orthoformate (0.32 mL, 2 mmol) was added with stirring over 5 min. The suspension was stirred until the uridine completely dissolved (~1 h), sodium bicarbonate (84 mg) was added, and the mixture was stirred for an additional 15 min. The suspension was filtered and the solid was washed with acetone. The filtrate and washings were combined and the solvent was removed in vacuo at 30 °C, giving crude 2′,3′-*O*-isopropylidene-[2′-^{13}C]uridine as a white solid: ^1H NMR (^2H_2O) δ 1.39 and 1.59 (s, 6 H, CH_3), 3.76 (dd, 1 H, H5″), 3.85 (dd, 1 H, H5′), 4.39 (m, 1 H, H4′), 4.90 (q, 1 H, H3′), 5.09 (dd, 1 H, H2′), 5.86 (d, 1 H, H5), 5.88 (dd, 1 H, H1′), 7.78 (d, 1 H, H6).

The crude 2′,3′-*O*-isopropylidene[2′-^{13}C]uridine was suspended in 15 mL of anhydrous tetrahydrofuran, triphenylphosphine (0.26 g, 1 mmol) and diethyl azodicarboxylate (0.18 mL, 1 mmol) were added, and the solution was stirred overnight at room temperature.[29] The solid precipitate (**8**) was collected by filtration and dried at 25 °C in vacuo: yield 0.07 g, 0.3 mmol, 30%; ^1H NMR (^2H_2O) δ 1.41 and 1.55 (s, 6 H, CH_3), 4.70 (dd, 1 H, H5′), 4.41 (dd, 1 H, H5″), 4.87 (d, 1 H, H4′), 5.25 (dd, 1 H, H3′), 5.15 (dd, 1 H, H2′), 5.84 (d, 1 H, H1′), 6.28 (d, 1 H, H5) and 7.93 (d, 1 H, H6).

Results and Discussion

Synthesis of ^{13}C-Labeled Ribonucleosides. The chemical synthesis of the ribonucleosides **1–4** has been accomplished with specific ^{13}C enrichment at C1′ and C2′ of the furanose ring (Figures 1–3). D-[^{13}C]Ribose, prepared by cyanohydrin reduction[15] and molybdate epimerization,[16] was coupled to acylated nitrogen bases (Table I) by using a modification of the Hilbert–Johnson reaction[30] developed by Vorbrüggen and co-workers.[24] Although other chemical and enzymic routes to prepare ribonucleosides have been reported,[31–33] the Vorbrüggen method appears to be most appropriate for the preparation of multigram quantities of stable isotopically labeled ribonucleosides that will be required for future structural studies of labeled oligonucleotides in this laboratory. Silylation of the nitrogen base with HMDS, followed by a Friedel–Crafts condensation with ^{13}C-labeled ABR

(25) Still, W. C. *J. Org. Chem.* **1978**, *43*, 2923.
(26) (a) Dekker, C. A. *J. Am. Chem. Soc.* **1965**, *87*, 4027. (b) Robbins, M. J.; Wilson, J. S.; Hansske, F. *J. Am. Chem. Soc.* **1983**, *105*, 4059.
(27) Verheyden, J. P. H.; Wagner, D.; Moffatt, J. G. *J. Org. Chem.* **1971**, *36*, 250.
(28) Tomasz, J. *Nucleic Acid Chemistry*; John Wiley and Sons: New York, Townsend, L. B., Tipson, R. S., Eds.; 1978; p 765.
(29) (a) Wada, M.; Mitsunobu, O. *Tetrahedron Lett.* **1972**, *13*, 1279. (b) Kimura, J.; Yagi, K.; Suzuki, H.; Mitsunobu, O. *Bull. Chem. Soc. Jpn.* **1980**, *53*, 3670.
(30) Hilbert, G. E.; Johnson, T. B. *J. Am. Chem. Soc.* **1930**, *52*, 4489.
(31) Fox, J. J.; Yung, N.; Davoll, J.; Brown, G. B. *J. Am. Chem. Soc.* **1956**, *78*, 2117.
(32) Hosono, A.; Fujii, K.; Tada, T.; Tanaka, H.; Ohgo, Y.; Ishido, Y.; Sato, T. *Bull. Chem. Soc. Jpn.* **1973**, *46*, 2818.
(33) (a) Frank-Kamenetskaya, M. D.; Knizhnikova, G. V.; Myasoyedov, N. F. *J. Radioanal. Nucl. Chem.* **1988**, *121*, 161. (b) For a recent review of nucleoside chemistry, see: *Chemistry of Nucleosides and Nucleotides*; Townsend, L. B., Ed.; Plenum Press: New York, 1988.

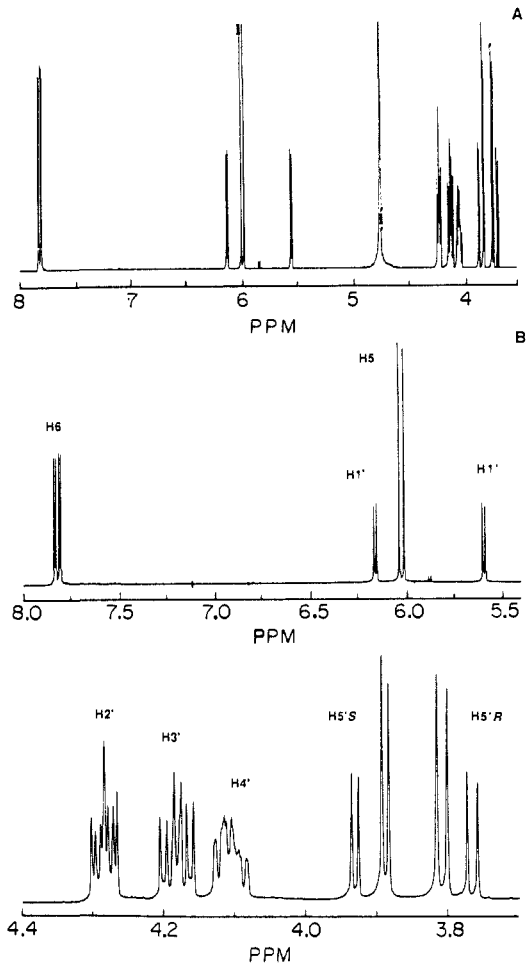

Figure 1. (A) The 300-MHz ^1H NMR spectrum of [1′-^{13}C]cytidine **2** in ^2H_2O. (B) Partial ^1H NMR spectrum of **2** showing the signals of H1′, H5, and H6. (C) Partial ^1H NMR spectrum of **2** showing the signals of H2′, H3′, H4′, H5′*R*, and H5′*S*.

and removal of the acyl protecting groups, gave the desired β-nucleoside in good yield. Two Lewis acid catalysts, stannic chloride and trimethylsilyl trifluoromethanesulfonate, were compared during this work. Use of stannic chloride produced an intractable emulsion during workup that made product isolation difficult; trimethylsilyl trifluoromethanesulfonate did not produce an emulsion and thus appears to be the reagent of choice.[24] Of the four ribonucleosides prepared, guanosine (**3**) was most difficult to synthesize and gave inconsistent yields of 20–65%. Although a careful study was not performed, the yield of **3** may depend on the base/sugar/catalyst ratio.[34]

An examination of the ^{13}C NMR spectra of the crude intermediate acylated ribonucleosides isolated after the Friedel–Crafts condensation revealed the presence of a minor byproduct characterized by a C1′ carbon signal slightly downfield of C1′ of the desired β-nucleoside. In the preparation of **1**, **2**, and **4**, this by product represented less than 3% (by NMR integration) of the total material, whereas in the preparation of **3**, this byproduct represented up to 14% of the total product. In the latter case, the byproduct was isolated and hydrolyzed with NH_3–MeOH and identified by ^{13}C and ^1H NMR spectroscopy as the N^7-linked nucleoside[35] in which the H-8, C-1′, C-4, and C-8 signals are shifted downfield relative to the corresponding signals in the N^9-linked isomer. Since the N^9-linked isomer is the thermodynamically controlled product,[36] an attempt was made to reduce the amount of N^7-linked nucleoside formed during the reaction by increasing the reaction time. However, increasing the reflux

(34) Lichtenthaler, F. W.; Voss, P.; Heerd, A. *Tetrahedron Lett.* **1974**, *24*, 2141.
(35) Garner, P.; Ramakanth, S. *J. Org. Chem.* **1988**, *53*, 1294.
(36) Vorbrüggen, H.; Höfle, G. *Chem. Ber.* **1981**, *114*, 1256.

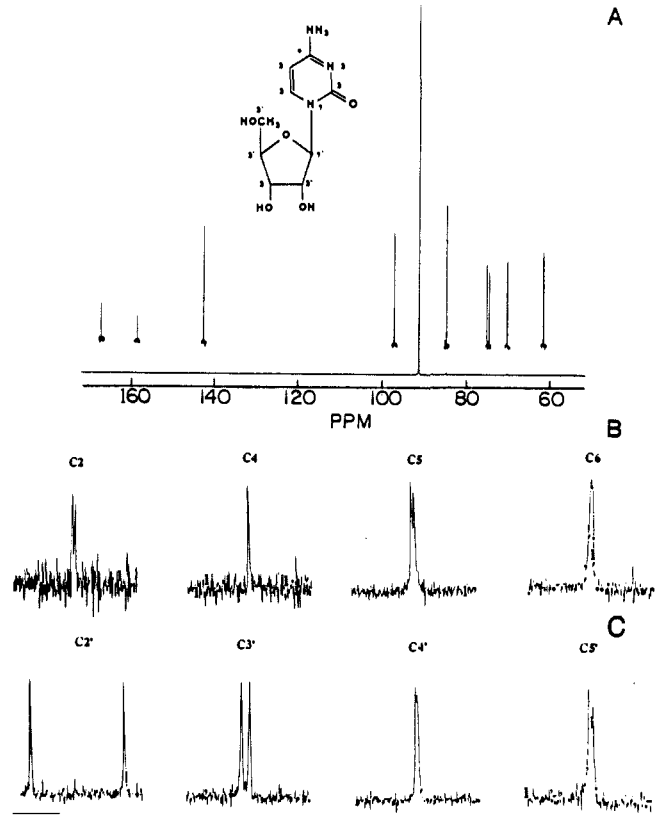

Figure 2. (A) The 75-MHz ^1H-decoupled ^{13}C NMR spectrum of [1′-^{13}C]cytidine **2** in ^2H_2O. (B) Expanded signals of the natural-abundance carbons of **2** showing the presence of ^{13}C–^{13}C spin coupling.

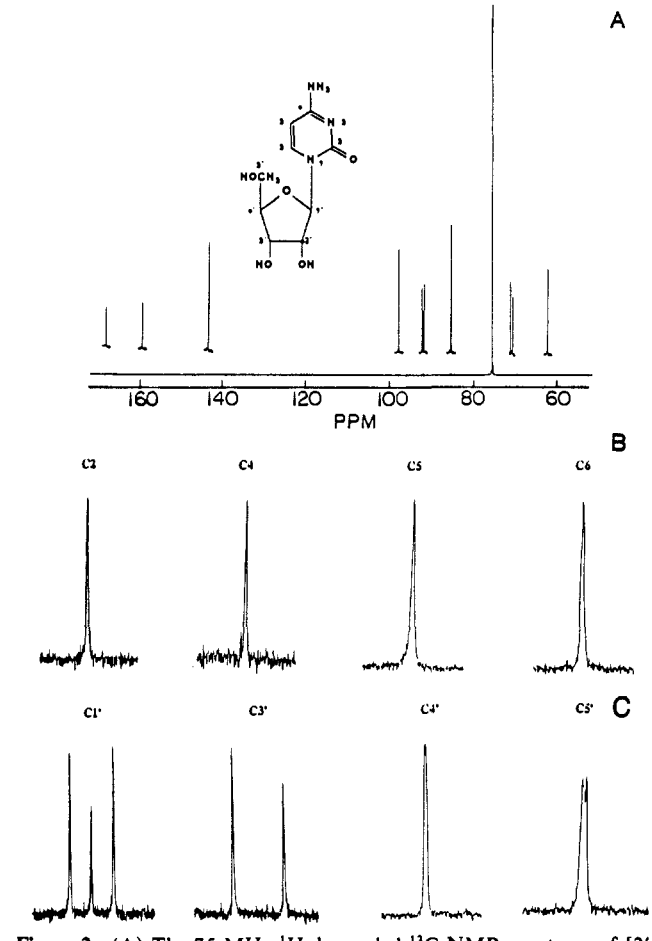

Figure 3. (A) The 75-MHz ^1H-decoupled ^{13}C NMR spectrum of [2′-^{13}C]cytidine **2** in ^2H_2O. (B) Expanded signals of the natural-abundance carbons of **2** showing the presence of ^{13}C–^{13}C spin coupling.

Table II. ^{1}H–^{1}H and ^{13}C–^{1}H Spin-Coupling Constants in Ribonucleosides and Methyl Ribofuranosides[a]

	adenosine[b] (1)	cytidine[b] (2)	guanosine[c] (3)	uridine[b] (4)	αR[e] (5)	βR[e] (6)
H1′,H2′	6.2	4.0	6.0	4.5	4.3	1.2
H2′,H3′	5.3	5.2	5.4	5.3	6.2	4.6
H3′,H4′	3.3	6.0	3.6	5.5	3.4	6.9
H4′,H5′*S*	2.8	2.8	3.1	2.9	3.3	3.1
H4′,H5′*R*	3.5	4.3	4.0	4.4	4.6	6.6
H5′*R*,H5′*S*	−12.8	−12.8	−12.8	−12.8	−12.4	−12.2
H5,H6		7.6		8.1		
C1′,H1′	165.6	170.3	165.6	170.1	173.3	174.2
C1′,H2′	3.2	1.7	~2.9	2.1	~0.6	0
C1′,H3′	~5.1	3.0	~4.7	3.5	4.6	0.9
C1′,H4′	1.3	0.6	1.3	0.7		3.0
C1′,H6		2.8		2.7		
C1′,H8	br[d]		br[d]			
C2′,H1′	3.2	3.5	3.3	3.1	2.2	br[d]
C2′,H2′	150.1	153.4	150.5	152.7	149.2	
C2′,H3′	0	0	0	0	1.1	1.4
C2′,H4′	1.6	1.1	1.6	1.3	0.8	0.7

[a] Values in hertz, accurate to ±0.1 Hz. [b] 50 mM in $^{2}H_2O$. [c] 2 mM in $^{2}H_2O$. [d] br denotes broadened resonance. [e] αR, methyl α-D-ribofuranoside; βR, methyl β-D-ribofuranoside. Assignments of H5′*R* and H5′*S* were taken from ref 11b.

Table III. ^{13}C–^{13}C Spin-Coupling Constants in Ribonucleosides and Methyl Ribofuranosides[a]

	adenosine[b] (1)	cytidine[b] (2)	guanosine[c] (3)	uridine[b] (4)	αR[e] (5)	βR[e] (6)
C1′,C2′	42.5	42.9	42.9	43.0	44.6	46.7
C1′,C3′	3.3	3.8	3.7	3.8	br[d]	3.1
C1′,C4′	0.8	0.8	br[d]	0.9	0	br
C1′,C5′	1.8	1.5	0	1.5	2.1	br
C1′,C2	0	1.3	0	1.9		
C1′,C5		1.4		1.4		
C1′,C6	0	0.7	0	0.4		
C1′,C4	0	0	0	0		
C1′,C8	1.8		0			
C2′,C3′	37.9	37.8	37.8	37.8	37.2	37.2
C2′,C4′	0.9	0.4	1.0	0.9	2.4	br[d]
C2′,C5′	0	1.6	0	1.6	0.9	1.5
C2′,C2	0	0	0	0		
C2′,C6	0	0	0	br[d]		
C2′,C4	0	0	0	0		
C2′,C8	0		0			

[a] Values in hertz, accurate to ±0.1 Hz. [b] 50 mM in $^{2}H_2O$. [c] 50 mM in DMSO-d_6. [d] br denotes broadened resonance. [e] αR, methyl α-D-ribofuranoside; βR, methyl β-D-ribofuranoside.

time from 4 to 48 h failed to significantly reduce the amount of N^7-linked nucleoside.

After deacylation, the labeled ribonucleosides were purified by column chromatography on Dowex 1 × 2 (200–400 mesh) resin in the OH^- form.[26] Adenosine (**1**) and cytidine (**2**) eluted with a methanol–CO_2-free water solvent; guanosine (**3**) and uridine (**4**) eluted with a triethylammonium bicarbonate buffer.

^{13}C–^{1}H and ^{13}C–^{13}C Coupling Constants in 1–4. ^{1}H–^{1}H, ^{13}C–^{1}H, and ^{13}C–^{13}C spin-coupling constants in **1**–**4** are given in Tables II and III. Spectra were obtained in $^{2}H_2O$ at 25 °C with the exception of the ^{13}C spectrum of **3**, which was obtained in DMSO-d_6. Several trends are apparent from an inspection of $J_{C,H}$ and $J_{C,C}$ values; the conformational implications of these trends are discussed later.

$^{1}J_{C1',H1'}$ depends on base structure, having a smaller value (165.6 ± 0.1 Hz) in purine ribonucleosides than in pyrimidine ribonucleosides (170.2 ± 0.2 Hz). $^{1}J_{C1',H1'}$ may be sensitive to *N*-glycoside bond conformation and dynamics according to recent studies by Davies and co-workers,[37] but the bicyclic, symmetric relationship between $^{1}J_{C1',H1'}$ and the *N*-glycoside torsion angle prevents the use of this coupling to establish *N*-glycoside conformation in the absence of additional structural information. Further complications in the interpretation of $^{1}J_{C1',H1'}$ arise from potential differences in the orientation of the C1′–H1′ bond (quasi-axial or quasi-equatorial); this orientation changes with ribofuranose conformation and may affect $^{1}J_{C1',H1'}$, which is expected to increase as the C1–H1 bond becomes more quasi-equatorial.[38]

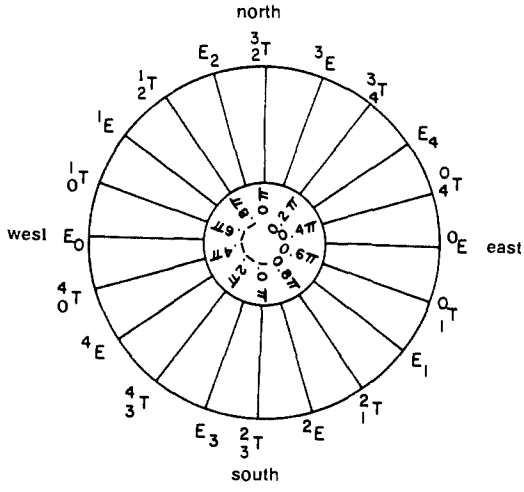

Figure 4. Pseudorotational itinerary of aldofuranose rings showing the pathway of interconversion between envelope (E) and twist (T) conformers. Envelope conformers have four ring atoms coplanar and one ring atom out-of-plane; twist conformers have three ring atoms coplanar and two ring atoms out-of-plane. Out-of-plane atoms are indicated by superscripts and subscripts.

$^{3}J_{C1',H4'}$ and $^{3}J_{C2',H4'}$ also depend on the structure of the nucleoside base. In pyrimidine nucleosides, $^{3}J_{C1',H4'} \cong 0.7$ Hz, while in purine nucleosides, $^{3}J_{C1',H4'} = 1.3$ Hz. $^{3}J_{C2',H4'}$ is less sensitive to base structure; **1** and **3** exhibit a coupling of 1.6 Hz while **2** and **4** show a coupling of ~1.2 Hz. $^{3}J_{C1',H3'}$ varies significantly with base structure, ranging from ~3.3 Hz in **2** and **4** to ~4.9 Hz in **1** and **3**.

In contrast to $^{1}J_{C1',H1'}$, $^{1}J_{C1',C2'}$ is relatively constant in **1**–**4** (42.8 ± 0.2 Hz), as expected since the β-configuration at C1′ is conserved in **1**–**4**. Previous studies of $^{1}J_{C1,C2}$ in structurally related aldofuranoses and aldofuranosides have shown this coupling to depend on anomeric configuration.[12,39]

$J_{C1',C3'}$ is also relatively constant in **1**–**4** (3.7 ± 0.2 Hz) and is determined by two competing coupling pathways, C1′–C2′–C3′ and C1′–O4′–C4′–C3′. Likewise, $J_{C1',C4'}$ is determined by two coupling pathways (C1′–C2′–C3′–C4′ and C1′–O4′–C4′) but is small in magnitude (~0.8 Hz); in comparison, no coupling is observed between C1 and C4 in simple aldofuranoses and aldofuranosides.[12,39c]

$^{3}J_{C1',C5'}$ lies in the range 1.5–1.8 Hz in **1**, **2**, and **4**, but is zero in **3**. $^{3}J_{C2',C5'} = 0$ Hz in the purine ribonucleosides **1** and **3**, while $^{3}J_{C2',C5'} = 1.6$ Hz in **2** and **4**. The conformational implications of these vicinal couplings are discussed below.

Several inter-ring couplings (i.e., couplings across the *N*-glycoside bond) are observed in [1′-^{13}C]- and [2′-^{13}C]ribonucleosides. In **2** and **4**, C1′ is coupled to H6 (2.7 ± 0.1 Hz); interestingly, H8 bears a similar relationship to C1′ in **1** and **3**, but only a small, unresolved coupling to C1′ is observed. C1′ is coupled to C8 in **1** (1.8 Hz) but not in **3**. In **2** and **4**, coupling is observed between C1′ and C6 (~0.6 Hz) and between C1′ and C5 (1.4 Hz). Vicinal coupling pathways exist between C2′–C4 and C2′–C8 of **1** and **3**, and between C2′–C2 and C2′–C6 in **2** and **4**, but in only one case ($^{3}J_{C2',C6}$ in **4**) is a small, unresolved coupling observed.

(37) (a) Davies, D. B.; MacCoss, M.; Danyluk, S. S. *J. Chem. Soc., Chem. Commun.* **1984**, 536. (b) Davies, D. B.; Rajani, P.; Sadikot, H. *J. Chem. Soc., Perkin Trans. 2* **1985**, 279.

(38) This expectation is based on the well-known relationship between $^{1}J_{C1,H1}$ and anomeric configuration in pyranosyl rings; axial C1–H1 bonds give a coupling of ~160 Hz, whereas equatorial C1–H1 bonds give a coupling of ~170 Hz: Bock, K.; Pedersen, C. *Acta Chem. Scand., Ser. B* **1977**, *B31*, 354.

(39) (a) Serianni, A. S.; Pierce, J.; Barker, R. *Biochemistry* **1979**, *18*, 1192. (b) Snyder, J. R.; Serianni, A. S. *Carbohydr. Res.* **1987**, *166*, 85. (c) Snyder, J. R.; Serianni, A. S. *Carbohydr. Res.* **1987**, *163*, 169.

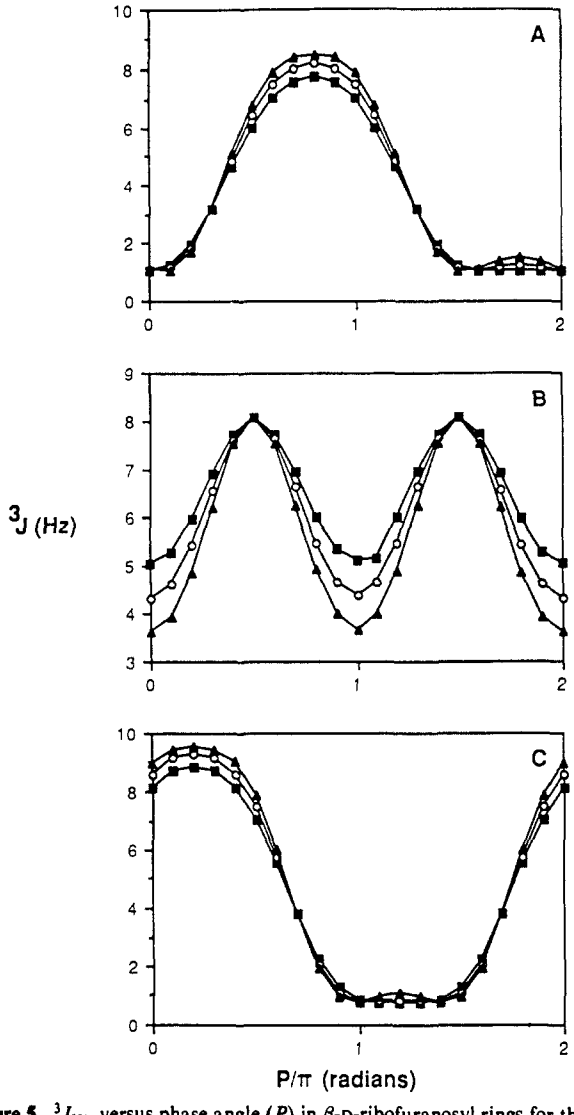

Figure 5. $^3J_{HH}$ versus phase angle (P) in β-D-ribofuranosyl rings for three puckering amplitudes. (a) $^3J_{H1',H2'}$. (b) $^3J_{H2',H3'}$. (c) $^3J_{H3',H4'}$. Puckering amplitudes: 35° (■), 40° (○), 45° (▲).

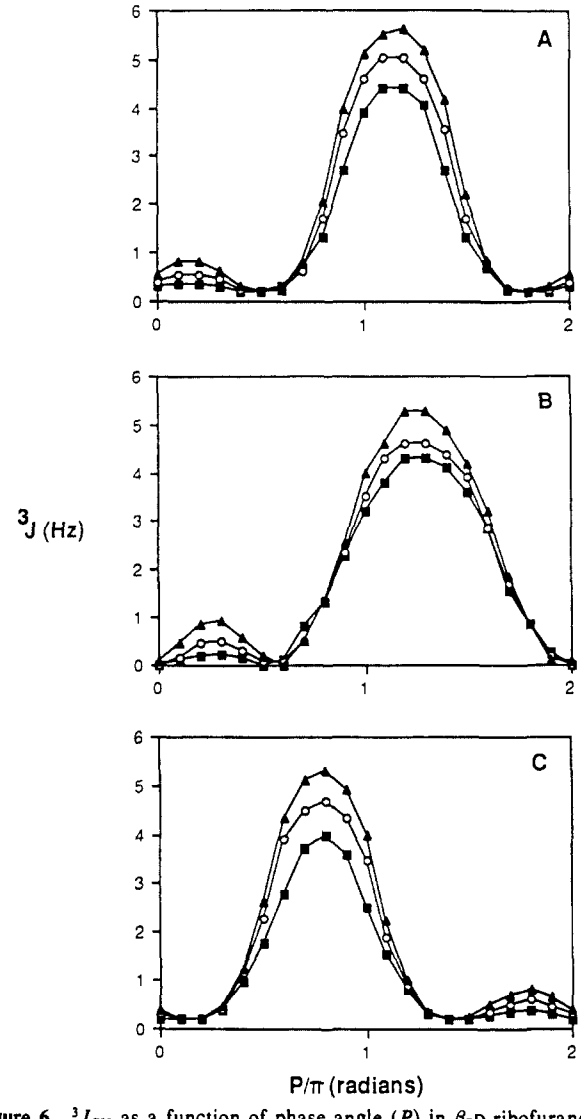

Figure 6. $^3J_{CH}$ as a function of phase angle (P) in β-D-ribofuranosyl rings. (a) $^3J_{C1',H3'}$. (b) $^3J_{C1',H4'}$. (c) $^3J_{C2',H4'}$. Puckering amplitudes: 35° (■), 40° (○), 45° (▲).

Ribofuranose Conformation in the Ribonucleosides 1–4. Vicinal ^1H–^1H spin-coupling constants ($^3J_{HH}$) are commonly used to evaluate furanose ring conformation in solution, although this method has limitations stemming from the well-documented conformational flexibility of the ring and the imprecise correlation between $^3J_{HH}$ and molecular dihedral angles.[40] Altona and Sundaralingam[41] have described furanose conformational dynamics using a pseudorotational itinerary (Figure 4) based on two parameters, phase angle (P) and puckering amplitude (τ_m). Phase angle defines the 20 idealized nonplanar conformers [10 envelope (E) and 10 twist (T) forms] and τ_m defines the out-of-plane displacement(s) (Figure 4). This itinerary provides a continuous pathway for the interconversion of nonplanar furanose conformers that does not include the planar form. An alternate pathway, known as inversion, describes nonplanar conformer interconversion via the planar form.

The application of three-bond (vicinal) coupling constants (^3J) to studies of molecular conformation requires a knowledge of Karplus curves appropriate to the molecular fragments under investigation. Dihedral angles of appropriate molecular fragments in the β-D-ribofuranose ring were calculated as a function of ring conformation by using the equations of de Leeuw et al.[42] These plots were converted to plots of $^3J_{HH}$ versus ring conformation (Figure 5) by using a generalized Karplus equation that accounts for substituent electronegativities and relative orientations.[43] Plots of ^3J versus furanose conformation for ^{13}C–C–C–^1H and ^{13}C–O–C–^1H coupling pathways (Figure 6) were generated from Karplus curves reported by Perlin and co-workers.[44,45] Although data are insufficient to construct similar curves for the C1′–C5′ and C2′–C5′ vicinal coupling pathways in β-D-ribofuranose, couplings of ~4.0 and ~1.5 Hz are reasonable estimates for 180° and 60° dihedral angles for the former pathway through the ring oxygen;[46,47] the C2′–C5′ pathway does not contain a heteroatom, and thus, smaller couplings are expected.

The analysis of ^3J values in furanoses is complicated by their potential conformational flexibility,[40] and an observed coupling constant may be consistent with a single conformation, a "virtual" conformation, or with several distinct conformations in rapid chemical exchange. The three intra-ring $^3J_{HH}$ values of the β-D-ribofuranose ring ($^3J_{H1',H2'}$, $^3J_{H2',H3'}$, $^3J_{H3',H4'}$) provide minimal

(40) Jardetzky, O. *Biochim. Biophys. Acta* **1980**, *621*, 227.
(41) Altona, C.; Sundaralingam, M. *J. Am. Chem. Soc.* **1972**, *94*, 8205.
(42) de Leeuw, F. A. A. M.; Van Kampen, P. N.; Altona, C.; Diez, E.; Esteban, A. L. *J. Mol. Struct.* **1984**, *125*, 67.
(43) (a) Haasnoot, C. A. G.; de Leeuw, F. A. A. M.; de Leeuw, H. P. M.; Altona, C. *Org. Magn. Reson.* **1981**, *15*, 43. (b) Haasnoot, C. A. G.; de Leeuw, F. A. A. M.; Altona, C. *Tetrahedron* **1980**, *36*, 2783.
(44) Schwarcz, J. A.; Perlin, A. S. *Can. J. Chem.* **1972**, *50*, 3667.
(45) Perlin, A. S.; Hamer, G. K. *Carbon-13 NMR in Polymer Science*; Pasika, W. M., Ed.; ACS Symposium Series 103; American Chemical Society: Washington, DC, 1979; p 123.
(46) Walker, T. E.; London, R. E.; Whaley, T. W.; Barker, R.; Matwiyoff, N. A. *J. Am. Chem. Soc.* **1976**, *98*, 5807.
(47) (a) King-Morris, M. J.; Serianni, A. S. *J. Am. Chem. Soc.* **1987**, *109*, 3501. (b) Snyder, J. R.; Serianni, A. S. *J. Org. Chem.* **1986**, *51*, 2694.

information to evaluate different conformational models. With ^{13}C enrichment at C1′ and C2′ of **1**–**4**, five $^3J_{CH}$ and $^3J_{CC}$ may be obtained to assist in conformational analysis; $^3J_{C1',H3'}$, $^3J_{C1',H4'}$, $^3J_{C2',H4'}$, $^3J_{C1',C5'}$, and $^3J_{C2',C5'}$.

A two-state model has been widely invoked to describe the conformational behavior of the β-D-ribofuranose ring in **1**–**4**. In this model, conformers clustered near ^3E (north conformers) and ^2E (south conformers) are assumed to be in rapid exchange via pseudorotation (Figure 4). Furthermore, ^0E (east) and E_0 (west) conformers do not contribute significantly to the total population, and north–south interconversion occurs predominantly through east conformers. This model is supported experimentally by X-ray crystallographic data[10] showing that the β-D-ribofuranose rings in crystalline ribonucleosides prefer conformations in either the north (N) or south (S) domains, and by potential energy calculations[8b] which show that conformers in these domains are more stable than those of the remaining itinerary. Potential energy calculations[8b] also show that the energy barrier for N–S interconversion is lower for the pathway involving east conformers. This two-state model provides the foundation for the NMR method of Altona and Sundaralingam[41,48] for estimating N and S populations in solution using $^3J_{H1',H2'}$ and $^3J_{H3',H4'}$. Altona and coworkers[43] have developed a parameterized Karplus equation to calculate theoretical $^3J_{HH}$ as a function of furanose ring conformation, which are used to fit observed $^3J_{HH}$ and compute the mole fractions of N and S conformers. This approach, however, may represent an oversimplification of β-D-ribofuranose conformational dynamics in solution. The two-state conformational model is based primarily on the statistical behavior of crystalline ribonucleosides where lattice forces may play a major role in stabilizing or destabilizing certain puckered conformers. In addition, solvation, especially in an aqueous environment with extensive hydrogen bonding, may affect furanose conformation and dynamics.

While there is reasonable support for the two-state model from potential energy calculations,[8b] it is important to recognize that the presence of east (^0E) and west (E_0) conformers in solution cannot be eliminated by the analysis of $^3J_{HH}$ data alone. However, an examination of $^3J_{C1',H4'}$ in **1**–**4** indicates that E_0 cannot be a major contributing form in solution, as a significant contribution by this conformer would produce a coupling constant larger than the one observed (0.6–1.3 Hz). This conclusion is particularly true for **2** and **4** where $^3J_{C1',H4'} < 0.7$ Hz. This example serves to illustrate the utility of $^3J_{CH}$, in certain circumstances, in evaluating potential conformational models.

By use of the simple formula, $K_{eq} = {}^sX/{}^nX = {}^3J_{H1',H2'}/{}^3J_{H3',H4'}$, derived by Davies and Danyluk[49] to estimate the relative proportions of north (^nX) and south (^sX) conformers, and $^3J_{HH}$ data in Table II, the following K_{eq} values are calculated: **1**, 1.9; **2**, 0.67; **3**, 1.7; **4**, 0.82. Thus, $^3J_{HH}$ data indicate an increased preference of N conformers in pyrimidine ribonucleosides.

$^3J_{C1',H4'}$, $^3J_{C1',H3'}$, and $^3J_{C2',H4'}$ in **1**–**4** can be examined for consistency with the above $^3J_{H,H}$ data. In converting the base from a purine (**1**, **3**) to pyrimidine (**2**, **4**), these couplings decrease in magnitude. The decrease in $^3J_{C1',H3'}$ (4.9 ± 0.3 to 3.3 ± 0.4 Hz) suggests a greater proportion of N conformers, since the dihedral angle between C1′ and H3′ decreases in these forms. The concomitant decreases in $^3J_{C1',H4'}$ (1.3 to 0.7 Hz) and $^3J_{C2',H4'}$ (1.6 to 1.2 Hz) (Table II), although smaller, nevertheless suggest a greater proportion of N conformers in **2** and **4**.

The greater proportion of N conformers in **2** and **4** compared to **1** and **3** as deduced from the above analysis of $^3J_{CH}$ values is also consistent with the larger values of $^3J_{C2',C5'}$ (~1.5 Hz) found in **2** and **4** relative to corresponding couplings in **1** and **3** (0 Hz) (Table III). The dihedral angle between C2′ and C5′ decreases from ~140° in ^3E (N conformer) to ~80° in ^2E (S conformer), and a larger $^3J_{C2',C5'}$ is expected in the former.

It has been suggested that methyl β-D-ribofuranoside (**6**) exhibits significantly different conformational behavior than the β-D-ribofuranose in ribonucleosides. Gerlt and Youngblood[50] proposed that **6** is ~60% ^3E conformer and ~40% ^2E conformer in aqueous solution. Cyr and Perlin[13] studied ^{13}C–^1H couplings in **6** and concluded that ^1E is the preferred conformation, whereas Serianni and Barker[12] suggested a mixture of E_2 and ^3E. $^3J_{CH}$ and $^3J_{CC}$ data (Tables II and III) suggest that **6** highly prefers N conformers near ^1E–E_2. In contrast to the ribonucleosides, $^3J_{C1,H3}$ and $^3J_{C2,H4}$ in **6** (~0.8 Hz) are significantly smaller than $^3J_{C1,H4}$ (3.0 Hz), as expected for N conformers. Observed couplings between C1 and C5 (<0.5 Hz), and C2 and C5 (1.5 Hz), are consistent with this conformational preference. By comparison, Cyr and Perlin[13] have proposed that methyl α-D-ribofuranoside (**5**) prefers an E_1 conformation, an S conformer. In contrast to **6**, $^3J_{C1,H3}$ (4.6 Hz) is significantly larger than $^3J_{C2,H4}$ (0.8 Hz) (Table II), and $^3J_{C1,C5}$ (2.1 Hz) is greater than $^3J_{C2,C5}$ (0.9 Hz) (Table III) in **5**. Thus, the available $^3J_{C,H}$ and $^3J_{C,C}$ values are consistent with a preferred conformation near E_1–^2E for **5** as deduced from $^3J_{H,H}$. Furthermore, it appears that the anomeric effect[51] plays a key role in determining preferred conformations of ribofuranosides, as both anomers prefer conformations that orient the C1–O1 bond quasi-axial or near-quasi-axial.

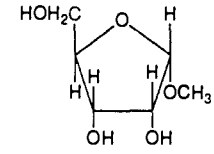

5

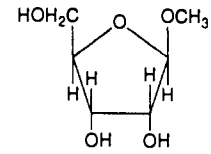

6

Coupling Constants in the Conformationally Constrained Nucleosides 7 and 8. Crystallographic studies[52,53] have shown that the furanose ring in 2,2′-anhydro-(1-β-D-arabinofuranosyl)uracil

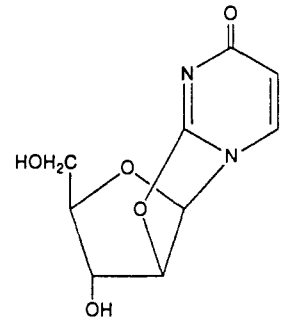

7

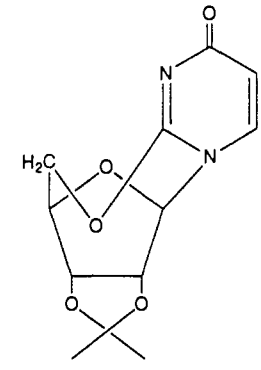

8

(**7**) assumes E_3–^4E conformations (south), whereas in 2′,3′-isopropylidene-2,5-*O*-cyclouridine (**8**), the furanose ring is fixed in the E_0 conformation (west). Similar conclusions were drawn from ^1H NMR studies of **7**[54] and **8**.[53] Consequently, these conformationally constrained nucleosides are useful models to assess the magnitudes of ^{13}C–^1H and ^{13}C–^{13}C couplings in furanose rings having fixed geometries.

In **7**, $^1J_{C1',H1'} = 185.4$ Hz, and $^1J_{C2',H2'} = 169.7$ Hz, and these couplings are considerably larger than those observed in **1**–**4** (~168 and ~152 Hz, respectively) (Table II). This difference is probably due in part to the geometric changes (strain) imposed by the anhydro ring (i.e., bond length and bond angle changes), although the enhanced value of $^1J_{C1',H1'}$ in **7** has been attributed previously to *N*-glycoside conformation.[37] Of particular interest

(48) Altona, C.; Sundaralingam, M. *J. Am. Chem. Soc.* **1973**, *95*, 2333.
(49) Davies, D. B.; Danyluk, S. S. *Biochemistry* **1974**, *13*, 4417.
(50) Gerlt, J. A.; Youngblood, A. V. *J. Am. Chem. Soc.* **1980**, *102*, 7433.
(51) (a) Edwards, J. T. *Chem. Ind. (London)* **1955**, 1102. (b) Lemieux, R. U.; Chii, N. J. *Abstracts of Papers*, 133rd National Meeting of the American Chemical Society, San Francisco, CA, April 1958, American Chemical Society: Washington, DC, 1958; 31N.
(52) (a) Suck, D.; Saenger, W. *Acta Crystallogr.* **1973**, *B29*, 1323. (b) Delbaere, L. T. J.; James, M. N. G. *Acta Crystallogr.* **1973**, *B29*, 2905.
(53) (a) Lemieux, R. U. *Ann. N.Y. Acad. Sci.* **1973**, *222*, 915. (b) Manor, P. C.; Saenger, W.; Davies, D. B.; Jankowski, K.; Rabczenko, A. *Biochim. Biophys. Acta* **1974**, *340*, 472.
(54) Cross, B. P.; Schleich, T. *Biopolymers* **1973**, *12*, 2381.

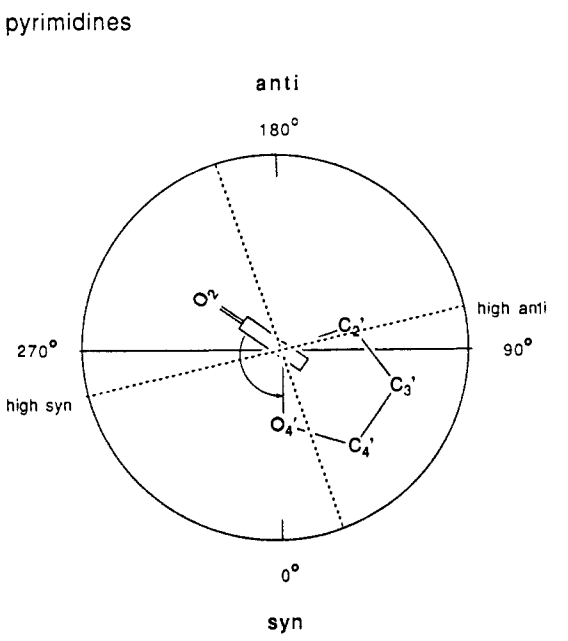

Figure 7. Conformational model for the *N*-glycoside bond in ribonucleosides (shown for pyrimidine bases). The conformational model proposed by Davies and co-workers[37b] comprises the four symmetric *N*-glycoside conformers denoted by the dashed lines.

are $^3J_{C1',H4'}$ (~5.2 Hz) and $^3J_{C1',H3'}$ (~3.4 Hz), which are consistent with dihedral angles of ~140° found in the E_3–^4E conformers.[55] $^3J_{C2',H4'}$ (~2.2 Hz) is smaller than expected for a dihedral angle of ~140°, but the Karplus relationship for this fragment may be affected by the anhydro ring and by the inverted configuration at C2' (relative to that in **1**–**4**). No coupling was observed between C2' and C5', as expected for a dihedral angle of ~90° in E_3–^4E conformers. $^3J_{C1',H6}$ = 1.7 Hz, a value considerably smaller than that observed in **2** and **4** (2.7 Hz); since the C1'–N1–C6–H6 torsion angle is the same (180°) in **2**, **4**, and **7**, other structural factors must be responsible for the difference. Several one- and two-bond couplings were also observed: $^1J_{C1',C2'}$ = 33.8 Hz, $^1J_{C2',C3'}$ = 41.5 Hz, $^2J_{C1',H2'}$ = 3.4 Hz, $^2J_{C2',H1'}$ = 2.4 Hz, and $^2J_{C2',H3'}$ = ~2.0 Hz.

Our NMR studies of **8** confirm the chemical shift assignments of H2' and H3' reported by Lemieux[53a] and refute those of Rabczenko and co-workers.[53b] In **8**, H2' resonates upfield of H3', as determined unequivocally from the ^{1}H NMR spectrum of the 2'-^{13}C-labeled compound in ^2H_2O or C^2HCl_3. $^1J_{C1',C2'}$ (43.8 Hz) and $^2J_{C2',H1'}$ (3.8 Hz) are comparable to corresponding couplings in **1**–**4** (43.0 and 3.3 Hz, respectively). On the other hand, $^1J_{C2',C3'}$ (30.9 Hz) is considerably smaller than corresponding values in **1**–**4** (~38 Hz), while $^1J_{C2',H2'}$ (165.2 Hz) and $^2J_{C2',H3'}$ (1.9 Hz) are larger than corresponding couplings in **1**–**4** (~152 Hz and no coupling, respectively). These data suggest that the eclipsed conformation about the C2'–C3' bond in **8** significant affects the magnitude of ^{13}C–^{1}H and ^{13}C–^{13}C couplings between nuclei defining this fragment. $^3J_{C2',H4'}$ = 3.6 Hz and is consistent with a dihedral angle of ~150° in the E_0 conformation. Likewise, $^3J_{C2',C5'}$ = 0 Hz, as expected for a dihedral angle of ~90° between these atoms in the E_0 conformer.

Coupling data collected on **7** and **8** point clearly to the fact that ^{13}C–^{1}H and ^{13}C–^{13}C couplings are affected by numerous factors,[55b] and conformational assignments based on any one of these couplings, in the absence of a quantitative understanding of its response to molecular structure, should be avoided. However, the observation of *trends* in these couplings in furanose rings of similar structure (e.g., the β-D-ribofuranose rings of **1**–**4**) is useful and can provide valuable information on conformational behavior.

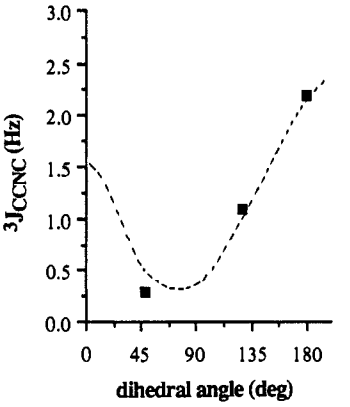

Figure 8. $^3J_{CCNC}$ versus torsion angle for the *N*-glycoside bond in ribonucleosides. Standard couplings were determined with the conformationally rigid nucleosides **7** and **8** (see text).

***N*-Glycoside Bond Conformation.** The *N*-glycoside torsion angle, χ, in nucleosides is defined by the O4'–C1'–N1–C2 pathway in **2** and **4**, and the O4'–C1'–N9–C8 pathway in **1** and **3**. Conformation about the C–N bond is divided into two broad ranges that characterize the syn and anti conformers, where syn = 0 ± 90° and anti = 180 ± 90° (Figure 7). In syn conformers of **2** and **4**, C2 is oriented over the ribose ring, while in anti conformers, C6 is oriented over the ring. In **1** and **3**, C4 is oriented over the ribose ring in syn conformers, whereas in anti conformers, C8 is oriented over the ring.

Several NMR methods have been developed to assess χ in **1**–**4**, including NOE measurements,[56] proton relaxation times,[57] chemical shift changes,[58] lanthanide ion probe techniques,[59] and $^3J_{CH}$ coupling constants.[37b,60] Lemieux and co-workers[60a] first described the use of $^3J_{C2,H1'}$ to evaluate *N*-glycoside conformation in pyrimidine ribonucleosides. In a subsequent study, Davies and co-workers[60b] concluded that both $^3J_{C2,H1'}$ and $^3J_{C6,H1'}$ must be measured to differentiate between syn and anti conformers. Davies et al.[37b] have proposed a four-state model of *N*-glycoside bond conformation, based on crystallographic studies of pyrimidine nucleosides, that involves equilibration between two syn and two anti conformers that are symmetrically related (Figure 7). Uridine was found to prefer χ torsion angles of 16° and 104° in the syn conformation and 196° and 284° in the anti conformation (Figure 7), the latter conformation being preferred (59%).

In this study, 2'-^{13}C-enriched **1**–**4** were used to evaluate the utility of $^3J_{CCNC}$ in estimating χ. A crude Karplus curve for the CCNC coupling pathway was constructed with two ^{13}C-enriched nucleoside derivatives having fixed (or highly constrained) values of χ: 2,2'-anhydro-(1-β-D-[2'-^{13}C]arabinofuranosyl)uracil (**7**) and 2',3'-isopropylidene-2,5'-*O*-[2'-^{13}C]cyclouridine (**8**). Crystallographic studies[52,53] of **7** and **8** provided an accurate evaluation of χ. In **7**, $^3J_{C2',C6}$ = 2.2 Hz and corresponds to a fixed C2'–C1'–N1–C6 torsion angle of 180°. In **8**, $^3J_{C2',C2}$ < 0.3 Hz and $^3J_{C2',C6}$ = 1.1 Hz, corresponding to C2'–C1'–N1'–C2 and C2'–C1'–N1–C6 torsion angles of 48° and 127°, respectively. Coupling

(55) (a) The presence of an oxygen atom in the coupling pathway is probably responsible for the fact that $^3J_{C1',H4'} > {}^3J_{C1',H3'}$ for similar dihedral angles; for example, in the conformationally rigid methyl β-D-gluco- and galactopyranosides, $^3J_{C1,H5}$ = 2.5 Hz and $^3J_{C1,H3}$ = 1.3 Hz for similar dihedral angles (~60°). See: Hayes, M. L.; Serianni, A. S.; Barker, R. *Carbohydr. Res.* **1982**, *100*, 87. (b) Marshall, J. L. *Carbon–Carbon and Carbon–Proton NMR Couplings: Applications to Organic Stereochemistry and Conformational Analysis*; Verlag Chemie: Weinheim, Germany, 1983.

(56) (a) Guêron, M.; Chachaty, C.; Tran-Dinh, S. *Ann. N.Y. Acad. Sci.* **1973**, *222*, 307. (b) Tran-Dinh, S.; Guschlbauer, W.; Guêron, M. *J. Am. Chem. Soc.* **1972**, *94*, 7903.

(57) (a) Imoto, T.; Akasaka, K.; Hatano, H. *Chem. Lett.* **1974**, 73. (b) Chachaty, C.; Perly, B.; Forchioni, A.; Langlet, G. *Biopolymers* **1980**, *19*, 1211.

(58) (a) Schweizer, M. P.; Banta, E. B.; Witkowski, J. T.; Robins, R. K. *J. Am. Chem. Soc.* **1973**, *95*, 3770. (b) Stolarski, R.; Dudycz, L.; Shugar, D. *Eur. J. Biochem.* **1980**, *108*, 111.

(59) (a) Barry, C. D.; North, A. C. T.; Glasel, J. A.; Williams, R. J. P.; Xavier, A. V. *Nature (London)* **1971**, *232*, 236. (b) Geraldes, C. F. G. C.; Williams, R. J. P. *Eur. J. Biochem.* **1978**, *85*, 463.

(60) (a) Lemieux, R. U.; Nagabhushan, T. L.; Paul, B. *Can. J. Chem.* **1972**, *50*, 773. (b) Davies, D. B.; Rajani, P.; MacCoss, M.; Danyluk, S. S. *Magn. Reson. Chem.* **1985**, *23*, 72.

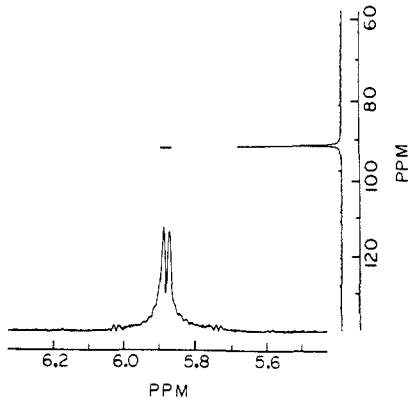

Figure 9. A 2D ^{13}C–^{1}H shift correlation map of [1′-^{13}C]uridine, showing the selective detection of the H1′ doublet via the enriched ^{13}C at C1′.

between C2′ and C2 in **7** (0 Hz) could not be used in the construction of the Karplus curve since it is affected by two pathways, C2′–C1′–N1–C2 and C2′–O2–C2. The crude Karplus curve constructed with three standard couplings is shown in Figure 8. The general shape and amplitude of this curve are similar to that predicted by Solkan and Bystrov[61] using FPT-INDO methods for the structurally related C_β–C_α–NH–CO pathway in peptides. The curve contains a minimum at a torsion angle of ~80°; the estimated amplitude at 0° is smaller than that at 180°, as expected from previous calculations.[61]

The observed values of $^3J_{C2',C2}$ and $^3J_{C2',C6}$ in **2** and **4**, and $^3J_{C2',C4}$ and $^3J_{C2',C8}$ in **1** and **3**, are small (Table III). Of the four most probable values of χ as deduced from studies of crystal structures[37b] (Figure 7), χ = 104° and χ = 284° should yield measurable couplings (~1.5–2.0 Hz) since dihedral angles of ~0° and ~180° are involved, whereas χ = 16° and χ = 196° should yield little or no coupling because of near-orthogonal dihedral angles. Thus, the ^{13}C–^{13}C coupling data across the *N*-glycoside bond in **1**–**4** are more consistent with preferred *N*-glycoside bond torsions with χ near 16° (syn) and near 196° (anti). This conclusion is consistent with results from semiempirical energy force field calculations on purine and pyrimidine ribonucleosides conducted by Pearlman and Kim[8c] that indicate preferred values of χ_{syn} = 12–24° and χ_{anti} = 222–236°, with interconversion taking place via the high anti conformation rather than via the high syn conformation (Figure 7). While the ^{13}C–^{13}C coupling data alone do not permit a quantitative evaluation of the syn–anti equilibrium or the preferred pathway of syn–anti interconversion in **1**–**4**, they are consistent with preferred syn and anti conformers in which the base is oriented approximately orthogonal to the C1–C2 bond in both conformations.

Implications for Structural Studies of More Complex Systems. A main motivation for conducting this study was to develop reliable chemical protocols to introduce ^{13}C and/or ^{2}H isotopes selectively into the furanose component of the ribonucleosides **1**–**4** in good yield[62] and to assess the utility of ^{13}C–^{1}H and ^{13}C–^{13}C spin couplings in the conformational analysis of these important biomolecules. Stable isotopically enriched **1**–**4** can be readily converted[26b,64] in good yield to the corresponding enriched 2′-deoxyribonucleosides,[65] which may be used in the assembly of selectively enriched DNA oligomers.[66] The presence of ^{13}C and ^{2}H enrichment in these oligomers is expected to simplify otherwise complex ^{1}H and ^{13}C NMR spectra, especially for larger fragments. For example, ^{13}C-enriched sites may be exploited in several multipulse NMR methods[47a,67] to obtain edited ^{13}C and ^{1}H NMR spectra of nuclei in the vicinity of the label, thereby allowing an inspection of local structure and conformation in oligomers as free entities or as components of molecular complexes. A simple application of this notion is illustrated in Figure 9. The 2D ^{13}C–^{1}H chemical shift correlation method applied to [1′-^{13}C]uridine and optimized for $^1J_{CH}$ permits the selective detection of the H1′ doublet, from which $^3J_{H1',H2'}$ may be readily measured; incorporation of a nucleotide monomer doubly enriched with ^{13}C at C2′ and C4′ into oligonucleotides should permit the selective detection of H2′ and H4′ of that monomer, thereby yielding all $^3J_{HH}$ within the pentofuranose ring.

Many pulse-editing techniques require prior knowledge of appropriate ^{13}C–^{13}C and ^{13}C–^{1}H spin couplings in order to be implemented, and several of these couplings have been accurately determined in this investigation. Several one-bond couplings (e.g., $^1J_{C2',C3'}$, $^1J_{C2',H2'}$) appear to be sensitive to furanose ring conformation and their utility in this regard deserves further investigation, as these couplings, due to their large magnitudes, should be more easily measured in complex structures. The small magnitudes of trans *N*-glycoside $^3J_{CCNC}$ values will probably limit their use to studies of *N*-glycoside conformation in small oligomers.

Acknowledgment. The grant support of the National Institutes of Health (GM 33791) and the Research Corporation (10028) is gratefully acknowledged.

(61) Solkan, V. N.; Bystrov, V. F. *Bull. Acad. Sci. USSR, Div. Chem. Sci.* **1974**, *23*, 1232.

(62) In this study the four labeled ribonucleosides **1**–**4** were prepared by condensing individual protected bases with labeled **ABR**. In practice, however, only **1**, **3**, and **4** require preparation by base–sugar condensation; **4** may be converted directly to **2** in good yield by treatment of the pertrimethylsilylated derivative with ammonia.[63]

(63) (a) Vorbrüggen, H.; Krolikiewicz, K.; Niedballa, U. *Ann. N.Y. Acad. Sci.* **1975**, *255*, 82. (b) Vorbrüggen, H.; Krolikiewicz, K.; Niedballa, U. *Annalen* **1975**, 988.

(64) Labeled thymidine is derived from labeled ribothymidine, which was not prepared in this study. However, ribothymidine can be obtained by a procedure siniilar to that used to prepare **4** but substituting silylated thymine for silylated uracil in the synthesis.

(65) Kline, P. C.; Serianni, A. S. *Magn. Reson. Chem.* **1990**, *28*, 324.

(66) (a) Manoharan, M.; Gerlt, J.; Wilde, J. A.; Withka, J. M.; Bolton, P. H. *J. Am. Chem. Soc.* **1987**, *109*, 7217. (b) Manoharan, M.; Ransom, S. C.; Mazumber, A.; Gerlt, J.; Wilde, J. A.; Withka, J. A.; Bolton, P. H. *J. Am. Chem. Soc.* **1988**, *110*, 1620.

(67) Brooks, W. M.; Irving, M. G.; Simpson, S. J.; Doddrell, D. M. *J. Magn. Reson.* **1984**, *56*, 521.